

Electrochemical Immunomagnetic Ochratoxin A Sensing: Steps Forward in the Application of 3,3',5,5'-Tetramethylbenzidine in Amperometric Assays

Soraya Höfs,^[a, b] Deniz Hülagü,^[c] Francesca Bennet,^[c] Peter Carl,^[a] Sabine Flemig,^[a] Thomas Schmid,^[a, d] Jörg A. Schenk,^[e] Vasile-Dan Hodoroaba,^[c] and Rudolf J. Schneider^{*,[a, f]}

Electrochemical methods offer great promise in meeting the demand for user-friendly on-site devices for monitoring important parameters. The food industry often runs own lab procedures, for example, for mycotoxin analysis, but it is a major goal to simplify analysis, linking analytical methods with smart technologies. Enzyme-linked immunosorbent assays, with photometric detection of 3,3',5,5'-tetramethylbenzidine (TMB), form a good basis for sensitive detection. To provide a straightforward approach for the miniaturization of the detec-

tion step, we have studied the pitfalls of the electrochemical TMB detection. By cyclic voltammetry it was found that the TMB electrochemistry is strongly dependent on the pH and the electrode material. A stable electrode response to TMB could be achieved at pH 1 on gold electrodes. We created a smartphone-based, electrochemical, immunomagnetic assay for the detection of ochratoxin A in real samples, providing a solid basis for sensing of further analytes.

1. Introduction

For food and feed safety, the monitoring of numerous contaminants such as mycotoxins plays a vital role since these fungal secondary metabolites can pose a severe health risk to humans and animals. The exposure of humans to mycotoxins occurs mainly through dietary intake.^[1] Thus, the European Commission has set legal limits for several mycotoxins such as ochratoxin A, deoxynivalenol, aflatoxins, patulin, zearalenone,

fumonisin and trichothecenes (e.g., T-2/HT-2 toxins^[2]). Ochratoxin A (OTA) is one of the most toxic and abundant mycotoxins. In animal and in *in vitro* experiments it was shown that OTA can be nephrotoxic,^[3] carcinogenic,^[3–4] neurotoxic^[5] and immunotoxic.^[6] For OTA, the legal limits in food and beverages are as low as a few $\mu\text{g kg}^{-1}$,^[2] and, consequently, analytical methods need to reach a low limit of detection. Therefore, many companies in food industry have their own laboratories to control mycotoxin contamination at the intake into their processes and at-line. Chromatographic methods such as high-performance liquid chromatography (HPLC)^[7] and gas chromatography (GC)^[7b,8] are frequently used to determine the OTA content in food and beverages.^[7–8] Furthermore, immunoanalytical methods, such as enzyme-linked immunosorbent assays (ELISA), are often applied.^[7d,9] They represent a less expensive alternative, but also rely on laboratory equipment and trained personnel. Thus, neither chromatographic methods nor ELISA are suitable for timely on-site analysis, so the demand for new, inexpensive, and user-friendly analytical approaches replacing laboratories remains high.

A system that works as simple as the prominent blood glucose meter expresses also great promise for future developments in food analysis.^[10] For blood glucose meters screen-printed enzyme electrodes are commonly used,^[11] in which the enzyme not only acts as the recognition element but also as signaling entity.^[10,11c] The enzymatic redox reaction is then typically detected by chronoamperometry.^[10] However, many analytes such as OTA or other mycotoxins cannot be quantified by enzymatic reactions, since there is no enzyme available which can perform a specific recognition and transformation. Consequently, other concepts were used to develop electrochemical OTA biosensors in which antibodies,^[12] aptamers^[13] or molecularly imprinted polymers (MIPs)^[14] act as the recognition elements, indispensably with very high affinity and selectivity

[a] S. Höfs, Dr. P. Carl, S. Flemig, Dr. T. Schmid, Dr. R. J. Schneider
Department of Analytical Chemistry; Reference Materials
Bundesanstalt für Materialforschung und -prüfung (BAM)
Richard-Willstätter-Straße 11, 12489 Berlin, Germany
E-mail: soraya.hoefs@bam.de
rudolf.schneider@bam.de


[b] S. Höfs
Institute for Biochemistry and Biology
University of Potsdam
OT-Golm, Karl-Liebknecht-Straße 24–25, 14476 Potsdam, Germany


[c] Dr. D. Hülagü, Dr. F. Bennet, Dr. V.-D. Hodoroaba
Department of Materials Chemistry
Bundesanstalt für Materialforschung und -prüfung (BAM)
Unter den Eichen 44–46, 12203 Berlin, Germany

[d] Dr. T. Schmid
School of Analytical Sciences Adlershof (SALSA)
Humboldt-Universität zu Berlin
Unter den Linden 6, 10099 Berlin, Germany

[e] J. A. Schenk
Hybrotec GmbH
Am Mühlenberg 11, 14476 Potsdam, Germany

[f] Dr. R. J. Schneider
Technische Universität Berlin
Straße des 17. Juni 135, 10623 Berlin, Germany

 Supporting information for this article is available on the WWW under <https://doi.org/10.1002/celec.202100446>

 © 2021 The Authors. ChemElectroChem published by Wiley-VCH GmbH. This is an open access article under the terms of the Creative Commons Attribution License, which permits use, distribution and reproduction in any medium, provided the original work is properly cited.

for the analyte. On the transduction side, many different electrochemical methods can be applied to develop electrochemical OTA detection systems. Electrochemical impedance spectroscopy was frequently exploited to develop label-free OTA sensors.^[12f,13a,b,15] In contrast to this, voltammetric techniques such as differential pulse voltammetry (DPV),^[12c] square wave voltammetry (SWV)^[12e] or amperometry^[12d] were applied for competitive immunosensors which operate very similarly to classical competitive immunoassays. Here the analyte competes with a labeled "tracer" molecule and subsequently the label is "quantified". Choosing an enzyme as label, the highly selective recognition of the tracer ("binding") is amplified via a high-turnover substrate reaction, and the product is detected at the electrode,^[12c-e] as is the case with ELISA (enzyme-linked immunosorbent assay).

Most ELISA systems are based on antibodies, proteins or haptens conjugated to horseradish peroxidase (HRP) and by far the most used HRP substrate for optical detection is 3,3',5,5'-tetramethylbenzidine (TMB) in combination with H₂O₂. This is attributed to the fact that TMB is a non-mutagenic chromogen which, due to the high turnover rates by HRP, provides high sensitivity in HRP-based assays.^[16] Josephy et al. described that the enzymatic oxidation of TMB by HRP in the presence of H₂O₂ initially generates a blue-colored charge-transfer complex existing in a rapid equilibrium with a radical cation which can further get oxidized to the yellow diimine.^[17] The formation of the yellow diimine can be accelerated by the addition of acids, such as H₂SO₄,^[18] and appears to be stable over time.^[17] It was shown that TMB is also electroactive and can be detected by voltammetric techniques in HRP-based immunoassays or sensors.^[19] In principle there are two possible electroactive species which can be quantified by reduction at an electrode after the enzymatic oxidation. One possibility is to detect the blue colored charge-transfer complex,^[20] and the other is to detect the yellow diimine after the addition of H₂SO₄.^[19d,g] Yet, only a few studies have been conducted to directly compare the electrochemistry of TMB at different pH values. In the study by Crew et al. it was demonstrated, by cyclic voltammetry on screen-printed carbon electrodes, that TMB undergoes a two-step oxidation and reduction at neutral pH, whereas a single two-electron oxidation and reduction is observed in the presence of H₂SO₄.^[19g]

Only limited research has been conducted on pitfalls in amperometric TMB detection, although it is well-known that oxidized TMB can form electroactive precipitates on electrode surfaces.^[21] For the application of electrodes in rapid test systems, the reproducibility of the electrochemical response is of great importance to ensure the reusability of one electrode for multiple measurements with reliable results. Since many established ELISAs are based on the TMB/H₂O₂ reaction with HRP, we believe that the optimization of the electrochemical detection of TMB can make an important contribution to the development of sensors and on-site detection systems for which important reagents (e.g. HRP hapten conjugates ("tracers") or HRP-labeled antibodies) already exist. We here compare the stability of the electrochemical redox reaction of TMB on gold and carbon screen-printed electrodes at weakly acidic

(pH 4) and highly acidic conditions (pH 1) by means of cyclic voltammetry. It is our aim to demonstrate the importance of the reaction conditions to the stability of the electrode response to TMB. Furthermore, we present the electrochemical behavior before and after the redox reaction with TMB and reveal conditions under which TMB residues remain on the electrode surface. The objective was to identify suitable reaction conditions for the electrochemical reduction of TMB. We demonstrate the suitability of the right conditions by an application in an immunomagnetic OTA assay with amperometric detection in a custom-made flow system. Finally, we applied our detection system to the analysis of OTA-spiked beer, the read-out performed with a smartphone connected via Bluetooth to a miniaturized potentiostat, providing a basis for on-site sensing of mycotoxins without conventional laboratory equipment.

2. Results and Discussion

2.1. Concept of the Immunomagnetic OTA Assay with Amperometric TMB Detection

A competitive immunomagnetic OTA assay has been developed, in which OTA competes with an OTA-HRP tracer for the antibody binding sites and subsequently the enzymatic reaction is detected amperometrically (see Figure 1). Magnetic particles, decorated with Protein G, were used to immobilize anti-OTA antibodies. Protein G provides a specific affinity to the Fc region of human, rabbit, mouse or goat immunoglobulin G (IgG) antibodies.^[22] This enables to control the orientation of the antibodies on the particles, with the paratopes exposed into the solution. Consequently, the functionalization of the particles with an anti-OTA antibody was performed by a single incubation step while shaking for 30 min. Afterwards, the beads were washed with buffer under magnetic capturing to remove unbound antibodies. In contrast to traditional ELISA formats, this assay format does not need the time-consuming overnight incubation step in which an antibody or protein conjugate is coupled to the surface of a microplate. In the next step, the anti-OTA antibody functionalized particles are incubated with different concentrations of OTA and an OTA-HRP tracer. Thereafter, several washing steps are conducted to remove unbound species. Finally, the HRP tracer converts added TMB. The oxidation product is indirectly proportional to the amount of bound OTA. H₂SO₄ is added after 20 min to stop the reaction and fully oxidize TMB which is either detected by photometry or by amperometry. The amperometric detection is performed with screen-printed gold electrodes in a custom-made flow system by sequentially injecting the samples into it after the enzymatic reaction was stopped. To miniaturize the detection system and to provide a low-cost alternative to expensive optical read-out systems, amperometric detection with a smartphone connected via Bluetooth to a small potentiostat was chosen.

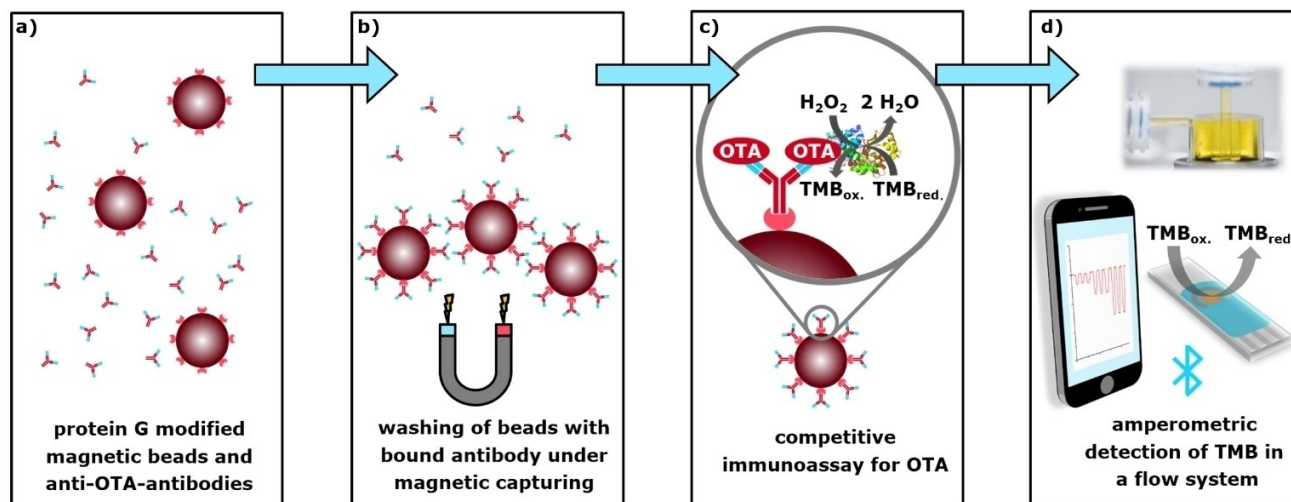


Figure 1. Schematic illustration of the immunomagnetic assay for OTA with amperometric TMB detection. **a)** Protein G modified magnetic beads are incubated with anti-OTA-antibodies and **b)** subsequently captured by a magnet and washed to remove unbound antibodies. Afterwards, **c)** antibody-decorated beads are applied to perform a competitive immunoassay for OTA in which OTA competes with an HRP-OTA tracer for the binding sites of the antibody. **d)** The amount of bound OTA is quantified by the enzymatic reaction of the HRP-OTA tracer with H_2O_2 and TMB. Enzymatically oxidized TMB is detected in the presence of H_2SO_4 by amperometry in a custom-made wall-jet flow cell. The signal read-out is performed with a smartphone which is connected via Bluetooth to a miniaturized potentiostat.

2.2. Cyclic Voltammetry of TMB on Gold and Carbon Screen-Printed Electrodes

For the enzymatic reaction of HRP with TMB/ H_2O_2 weakly acidic pH values (pH 5–6) are well-suited to obtain a high reaction rate.^[16a] However, it was reported that dissolved TMB is less likely to precipitate at pH 4 in sodium citrate buffer than in various other buffer systems with pH values ranging from 5 to 6.^[23] To prevent precipitation, the HRP reaction with TMB/ H_2O_2 for the OTA assay was performed at pH 4 in sodium citrate buffer. It should be noted here that the ability of TMB to form precipitates has also been exploited in sensorial systems by detecting an electroactive precipitate on electrode surfaces after oxidation with HRP.^[21a] However, for successive measurements, such a reaction might be disadvantageously since precipitates on electrode surfaces will change their response over time. Consequently, we studied the stability of the electrochemical reaction of TMB by cyclic voltammetry at different pH values (pH 4 and pH 1) and at two electrode materials (gold and carbon) to identify conditions, which allow a stable electrode response in consecutive measurements.

To assess the stability of the electrochemical reaction of TMB at carbon and gold electrodes at pH 4, 30 cycles of cyclic voltammetry were performed with both electrode materials (see Figures 2a and d). For both types of electrodes, two oxidation and reduction peaks were detected, indicating that the redox reaction of TMB occurs in two steps. This was also reported in other studies on gold electrodes at pH values ranging from 5 to 7.4.^[21b,24] On carbon, the two oxidation peaks have peak potentials of 0.21 V and 0.47 V vs. Ag/AgCl and the reduction peak potentials were found at 0.4 V and 0.16 V vs. Ag/AgCl. For the gold electrode, similar oxidation and reduction peak potentials of 0.23 V, 0.43 V vs. Ag/AgCl and 0.36 V, 0.18 V

vs. Ag/AgCl, respectively, were identified. This illustrates that a comparable electrochemical response of TMB occurs at both electrode materials. Furthermore, we observed that for both electrodes the redox currents decrease with the number of scans and after 30 cycles a dark blue precipitate could be spotted on the electrode surfaces. After 30 cycles the electrodes were rinsed with sodium citrate buffer (pH 4) to remove the visible precipitates. Subsequently, cyclic voltammetry in buffer without TMB was performed again and compared to measurements obtained in buffer of the unused electrodes to test whether the response has changed by the electrochemical reaction with TMB (see Figures 2b and e). It was found that an electrochemical response of TMB can still be detected for both electrode types, which leads to the conclusion that TMB remains partially at the electrode surfaces.

To verify these results, Raman microspectroscopy of the electrode surfaces was performed according to Schmid and Dariz^[25] (see Figures S14 and S15). When large TMB precipitates are not removed from the electrode surfaces, characteristic Raman spectra of oxidized TMB were obtained, which are in good agreement with those described in literature.^[18] On the gold surfaces some local residues of TMB precipitates could be also identified after carefully rinsing the electrodes with ultrapure water (see Figure S14d) confirming the results obtained by cyclic voltammetry. For the carbon electrodes it was not possible to detect small residues of TMB precipitates after rinsing the electrodes with ultrapure water (see Figure S15d). This can be most likely attributed to adsorption of significant amounts of TMB inside the porous material along with the small penetration depth of Raman measurements limited by optical absorption and scattering, whereas the gold electrode provides a rather reflective surface to this technique.

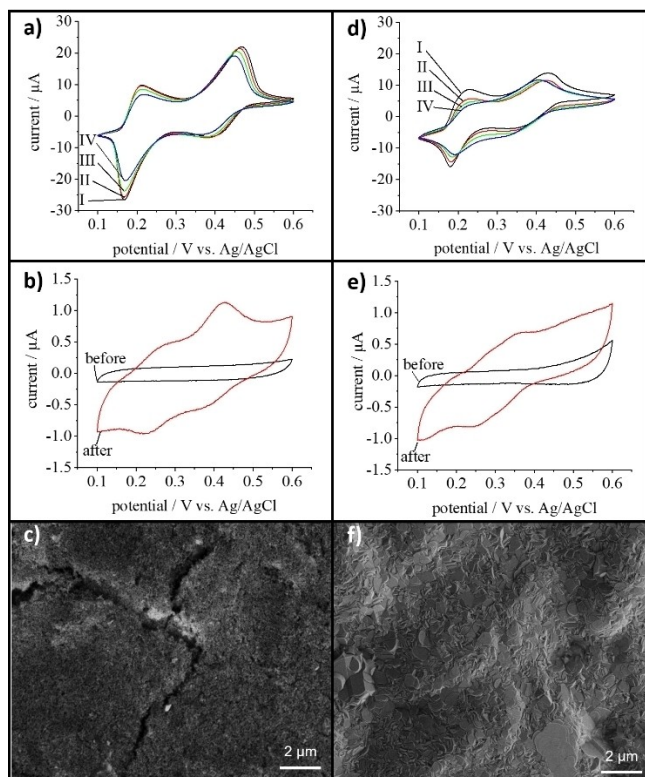


Figure 2. Cyclic voltammetry of TMB at pH 4 at a scan rate of 100 mV s^{-1} on carbon and gold screen-printed electrodes and the corresponding SEM images. **A)** Cycle 2 (I), 10 (II), 20 (III) and 30 (IV) performed in $500 \mu\text{M}$ TMB at pH 4 in 220 mM sodium citrate buffer with 100 mM KCl at a screen-printed carbon electrode. **b)** Results obtained with the same electrode at pH 4 in 220 mM sodium citrate buffer with 100 mM KCl without TMB in solution before and after 30 cycles in TMB were performed. **c)** SEM image of the surface of the carbon screen-printed electrode after the electrochemical measurements presented in a) and b) at an acceleration voltage of 5 kV . **d)** Cycle 2 (I), 10 (II), 20 (III) and 30 (IV) performed in $500 \mu\text{M}$ TMB at pH 4 in 220 mM sodium citrate buffer with 100 mM KCl at a screen-printed gold electrode. **e)** Results obtained with the same electrode at pH 4 in 220 mM sodium citrate with 100 mM KCl without TMB in solution buffer before and after 30 cycles in TMB. **f)** SEM image of the surface of the gold screen-printed electrode after the electrochemical measurements presented in d) and e) at an acceleration voltage of 5 kV .

To characterize the surface morphology of the electrodes, scanning electron microscopy (SEM) was performed for both working electrodes after the electrochemical treatment. By SEM, a porous surface with some larger cracks of a few hundred nanometers was observed for the carbon electrode (see Figure 2c), whereas the gold electrode provides a non-porous closed structure (Figure 2f). However, in comparison to unused electrodes, no significant morphological differences could be observed which suggests that no larger TMB precipitates adhere to the electrode surfaces (cf. Figures S1 and S2). To further evaluate if TMB was deposited on the electrode surface the elemental composition of the carbon electrodes was analyzed before and after the electrochemical measurements by energy dispersive X-ray spectroscopy (EDS), since the deposition of TMB would lead to more nitrogenous compounds on the electrode surface. No significant difference could be detected in the nitrogen content and the elemental composi-

tion of both electrode materials (see Figure S5). This confirms the absence of larger TMB deposits at the electrode surface. However, to reveal very small differences in the chemical composition at the surface, the sensitivity achieved by EDS ($\sim 1 \text{ wt}\%$ for nitrogen) might be not sufficient.

Hence, the surface of the carbon electrode was analyzed by Time-of-Flight–Secondary Ion Mass Spectrometry (ToF-SIMS, with an IONTOF ToF-SIMS IV instrument) which analyzes the composition of the upper atomic layers of the surface of a material with an extremely high sensitivity. The principal component analysis of the ToF-SIMS data of a TMB-exposed electrode surface in comparison to an unused electrode could not identify any TMB residues (see Supporting Information). Also, with this method, we could not determine any increased nitrogen content. Hence, the results suggest that the remaining redox reaction of the electrode in buffer after rinsing might not be associated with TMB precipitates on the upper surface of the electrode, but rather by TMB which might remain at a deeper level in pores or cracks of the carbon electrode. For detailed information, see Supporting information. In summary it can be stated that neither carbon nor gold electrodes provide stable redox currents in the electrochemical reaction with TMB at pH 4. Hence, we repeated the cyclic voltammetry with both electrode types after the addition of H_2SO_4 to TMB at pH 1.

At pH 1 a completely different electrochemical response of TMB is observed. For the carbon and the gold electrode only one sharp oxidation and reduction peak can be observed at 0.48 V and 0.43 V vs. Ag/AgCl, respectively (see Figures 3a and d). This indicates that the oxidation as well as the reduction of TMB occur in a single step. Furthermore, a stable signal with no decrease of the redox current was obtained in cyclic voltammetry over 30 cycles and no precipitates could be found after 30 cycles. However, after rinsing the carbon electrode with buffer (with H_2SO_4 , pH 1), small redox currents can still be detected, indicating that also under these conditions a proportion of TMB remains at the electrode. In contrast to this, no redox current can be observed at the gold electrode after rinsing it with buffer. The charging currents of the electrode are almost identical before and after the TMB treatment. The electrode response in buffer is not affected by the previous electrochemical reaction with TMB. Furthermore, we could confirm by Raman spectroscopy that the spectrum of the TMB exposed gold electrode shows no significant difference to a spectrum obtained for a bare gold electrode (see Figures S14f and h). The electrode surfaces were also characterized by SEM and a similar surface morphology of the electrodes as described above was found (see Figures 3c and f). Also, here, the working electrodes show no significant difference relative to the unused electrodes (see Figure S1). The results suggest that the remaining redox response of TMB at carbon electrodes at pH 1 might be caused by TMB remaining in the deep porous structure, whereas the closed structure of the gold electrode might facilitate the removal of the redox species.

To further study the electrochemistry of TMB at pH 1 on gold electrodes, cyclic voltammetry with different scan rates was performed (see Figure 4). It could be clearly demonstrated that both, the anodic and the cathodic peak potentials (E_p , and

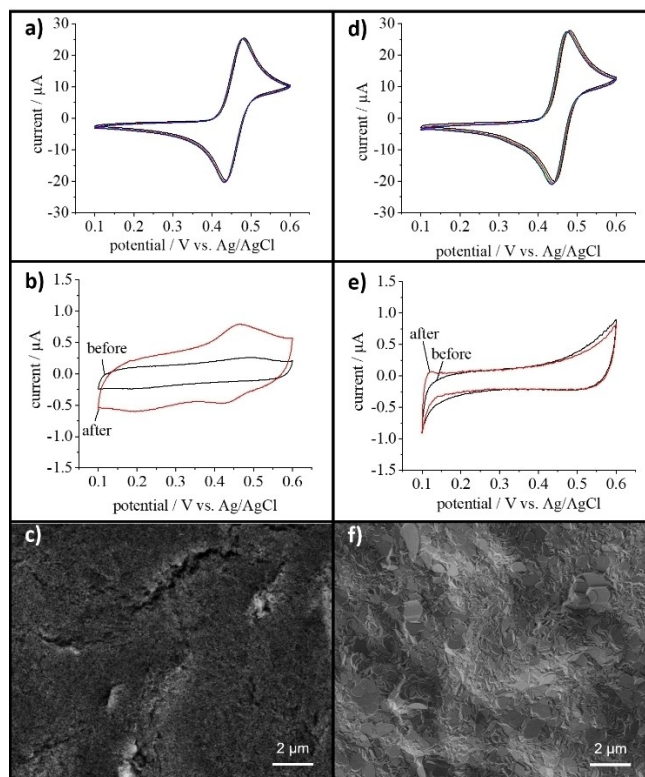


Figure 3. Cyclic voltammetry of TMB at pH 1 at a scan rate of 100 mV s^{-1} on carbon and gold screen-printed electrodes and the corresponding SEM images. **a)** Cycle 2 (I), 10 (II), 20 (III) and 30 (IV) performed in $500 \mu\text{M}$ TMB at pH 1 in 150 mM sodium citrate buffer with 300 mM H_2SO_4 and 100 mM KCl at a screen-printed carbon electrode. **b)** Results obtained with the same electrode at pH 1 in 150 mM sodium citrate buffer with 300 mM H_2SO_4 and 100 mM KCl without TMB in solution before and after 30 cycles in TMB were performed. **c)** SEM image of the surface of the carbon screen-printed electrode after the electrochemical measurements presented in **a)** and **b)** at an acceleration voltage of 5 kV . **d)** Cycle 2 (I), 10 (II), 20 (III) and 30 (IV) performed in $500 \mu\text{M}$ TMB at pH 1 in 150 mM sodium citrate buffer with 300 mM H_2SO_4 and 100 mM KCl at a screen-printed gold electrode. **e)** Results obtained with the same electrode at pH 1 in 150 mM sodium citrate buffer with 300 mM H_2SO_4 and 100 mM KCl without TMB in solution before and after 30 cycles in TMB. **f)** SEM image of the gold screen-printed electrode after the electrochemical measurements presented in **d)** and **e)** at an acceleration voltage of 5 kV .

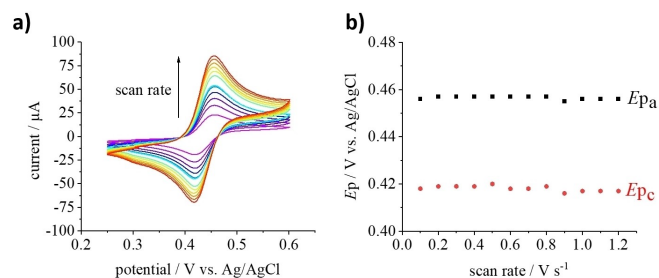


Figure 4. **a)** Cyclic voltammetry with scan rates ranging from 0.1 – 1.2 V s^{-1} performed in $500 \mu\text{M}$ TMB at pH 1 in 150 mM sodium citrate buffer with 300 mM H_2SO_4 and 100 mM KCl at a screen-printed gold electrode. **b)** Peak potentials (E_p) obtained for the anodic (E_{p_a}) and cathodic peak (E_{p_c}) vs. the scan rate.

E_{p_c}), are not a function of the scan rate, indicating a rather reversible character of the reaction. Additionally, the peak

current ratio of the anodic and cathodic current was determined to be near unity over to whole investigated scan rate range. The peak currents are a linear function of the square root of the scan rate, indicating a diffusion-controlled reaction (see Figure S16). To the best of our knowledge this scan rate depended characterization of TMB at highly acidic pH values has not yet been reported in literature. A formal potential of $0.437 \pm 0.001 \text{ V}$ vs. Ag/AgCl was determined, which is relatively similar to the formal potential of 0.452 V vs. Ag/AgCl for TMB at highly acidic conditions reported by Fanjula-Bolado et al.^[19d] Overall, the rather reversible character of the reaction and the stability of the redox reaction are beneficial for the analytical quantification of TMB. Therefore, we decided to perform the analytical detection of oxidized TMB in the OTA assay with gold electrodes at pH 1 (in the presence of H_2SO_4).

2.3. Comparison of Different Antibodies by ELISA

For the development of the magnetic bead-based OTA assay three different anti-OTA mouse IgG antibodies (BG4, BC10 and CH2) were tested by ELISA for their sensitivity. Therefore, a direct competitive assay format was selected. Primarily, an OTA-HRP tracer was synthesized by activating the carboxylic group of OTA by DCC/NHS chemistry and subsequent coupling to the amino groups of the enzyme. By matrix-assisted laser desorption/ionization time-of-flight mass spectrometry (MALDI-TOF/MS) it was found that approximately one OTA molecule has bound per enzyme (see Figure S17). For the ELISA a secondary rabbit anti-mouse IgG antibody was bound to the surface of a microplate to capture the primary anti-OTA mouse antibodies. A competitive reaction between the OTA and an OTA-HRP tracer is then performed and after removing the unbound species, TMB/ H_2O_2 is added to quantify the OTA concentration by the enzymatic reaction (see Figure 5a). The C-value, which is the inflection point of the obtained curve was used to compare the sensitivity achieved in the ELISAs with three different antibodies. For the BG4 antibody a C-value of $1.26 \pm 0.03 \text{ nM}$ was obtained, which is about one order of magnitude lower than those obtained for the two other antibodies ($C_{\text{BC10}} = 10.7 \pm$

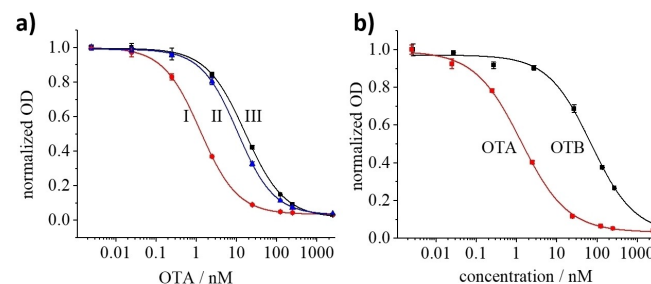


Figure 5. **a)** ELISA for Ochratoxin A for the comparison of different mouse IgG anti-OTA antibodies obtained from different cell clones (I) BG4 (II) BC10 (III) CH2. The obtained C-values were: $C_{\text{BG4}} = 1.26 \pm 0.03 \text{ nM}$; $C_{\text{BC10}} = 10.7 \pm 0.4 \text{ nM}$; $C_{\text{CH2}} = 16.5 \pm 0.7 \text{ nM}$. **b)** ELISA for Ochratoxin A and Ochratoxin B with the BG4 antibody. A cross-reactivity of 1.8% was calculated. C-Values were $C_{\text{OTA}} = 1.3 \pm 0.1 \text{ nM}$, $C_{\text{OTB}} = 72 \pm 13 \text{ nM}$. Error bars were obtained from four independent measurements.

0.4 nM; $C_{\text{CH}_2} = 16.5 \pm 0.7$ nM). Thus, we continued working with the BG4 antibody for all further experiments.

In food samples, OTA often occurs simultaneously with the non-chlorinated Ochratoxin B (OTB), which is less toxic than OTA.^[26] For an analytical test system, it is therefore of great importance to distinguish between OTA and OTB. We have thus determined the cross-reactivity of the BG4 antibody with OTB and found that it is only 1.8% (see Figure 5b). It was therefore possible to demonstrate that the BG4 antibody not only achieves good sensitivity, but also discriminates between OTA and OTB.

2.4. Immunomagnetic OTA Assay with Amperometric Detection

Protein G decorated magnetic beads with a diameter of about 2.8 μm were used to develop a magnetic bead-based OTA assay (see Figure S18). This enables on the one hand to shorten the overall assay time and on the other hand to perform the assays also on other platforms than the microplate. The BG4 antibody was applied to develop the assay on magnetic beads, which is similar to the ELISA described above. However, due to the protein G coating of the beads no secondary antibody is required.

To develop an application-oriented detection method which can be miniaturized for on-site measurements, we have developed an electrochemical detection system to quantify enzymatically oxidized TMB after the addition of H_2SO_4 . A custom-made wall-jet flow cell was developed and fabricated by poly(methyl methacrylate) (see Figures S19 and S20), to conduct electrochemical measurements with the screen-printed gold electrodes under continuous flow of the solution. The flow cell allows to sequentially inject the samples from the magnetic bead-based assay. To test the flow cell, amperometric measurements with $\text{K}_3[\text{Fe}(\text{CN})_6]$ were performed (see Figure S21). A linear relation between the concentration and current response and high repeatability were achieved, demonstrating that the flow cell is well-suited for analytical amperometric measurements.

To detect oxidized TMB for the OTA assay, amperometry was performed at a fixed potential, which is sufficiently low to reduce TMB. From cyclic voltammetry it could be observed that oxidized TMB can be reduced at quite positive potentials which are below the formal potential of 0.437 V vs. Ag/AgCl (see Figure 4a). To obtain a stable diffusion controlled current, a potential of 300 mV vs. Ag/AgCl was applied in amperometric measurements. Since the screen-printed gold electrodes are combined on one chip with a platinum counter electrode and a silver pseudo-reference electrode, it is inevitable to use a high Cl^- concentration to stabilize the potential of the reference electrode. The use of 0.1 M KCl as an additive in the buffer and in each sample has been found to be well-suited. To detect the enzymatically oxidized TMB after the addition of H_2SO_4 , the amperometric reduction must be performed in the presence of all the other enzymatic substrates and products. To avoid possible interferences, the influence of the H_2O_2 and TMB

substrate solution on the amperometric signal was tested at 300 mV vs. Ag/AgCl. It was found that both, H_2O_2 and TMB, give a small current signal of a few nA (see Figure S22). Thus, we have added H_2O_2 and TMB to the running buffer. Figures 6a and 6b show the results of the amperometric detection for the quantification of OTA. The sensitivity of the magnetic bead-based assay is similar as for the classical ELISA ($C = 2.1 \pm 0.3$ nM). To compare the electrochemical detection method with the traditional optical TMB detection, the OD of each sample was measured. It was found that both methods provide the same sensitivity and are in good correlation (see Figures 6c and d).

To demonstrate the applicability of our electrochemical OTA detection system, measurements in OTA-spiked beer were performed. Hitherto, no legal limits for OTA in beer have been set by the European Commission. However, it has already been announced in the COMMISSION REGULATION (EC) No 1881/2006 that setting a maximum level for OTA in beer is under consideration.^[2] Therefore, the influence of the complex sample matrix under different dilutions with buffer (1:1; 1:5 and 1:10) was tested in the magnetic bead-based assay with optical detection (see Figure 7a). It was found that with higher beer content the signal intensity as well as the sensitivity of the assay decreases. This indicates that the matrix influences the binding of the antibody to OTA, which might be associated with the ethanol content or other interfering species of the matrix. With OTA standard solutions a maximum OD signal of approximately 1 and a C-value of 1.25 ± 0.14 nM was obtained. Under these optimized assay conditions, a limit of detection of 150 pM is achieved, which equals an OTA content of 60 ng L^{-1} . For the 1:1 diluted beer sample the maximum OD intensity is

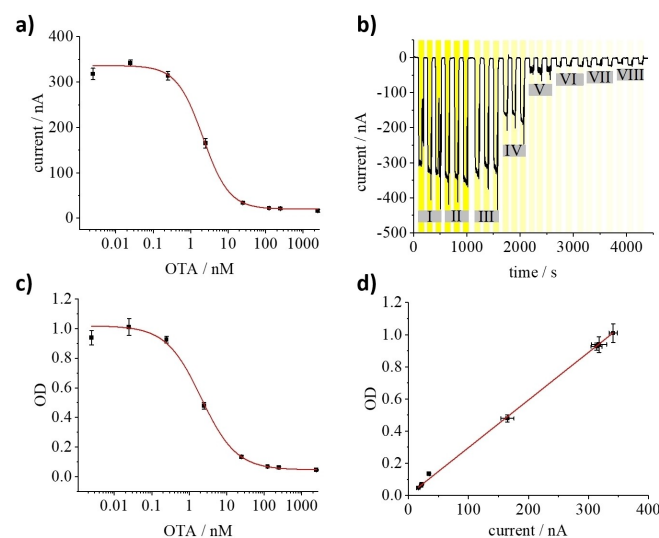


Figure 6. a) Results of the immunomagnetic OTA assay with amperometric detection of TMB ($C = 2.1 \pm 0.3$ nM) b) Amperometric curve measured at 300 mV vs. Ag/AgCl with a flow rate of $600 \mu\text{L min}^{-1}$ in 150 mM sodium citrate buffer with 300 mM H_2SO_4 and 100 mM KCl (pH 1). For each OTA concentration three independent samples were measured (I 2.5 pM II 25 pM III 250 pM IV 2.5 nM V 25 nM VI 124 nM VII 250 nM VIII 2.5 μM). c) Results of the same immunomagnetic assay measured by photometry ($C = 2.1 \pm 0.3$ nM) and d) the correlation of both detection techniques. Error bars were obtained from three independent measurements.

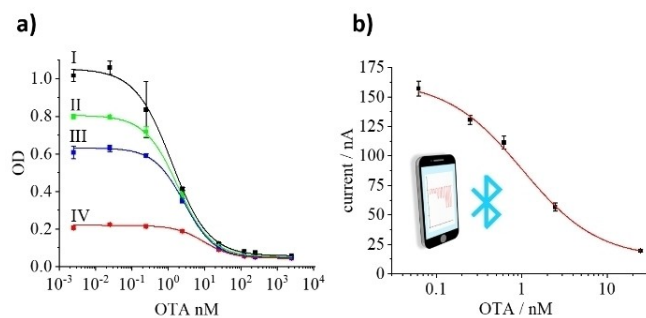


Figure 7. a) Immunomagnetic OTA assay with different dilutions of OTA-spiked beer (with Tris buffer) and photometric TMB detection (I – without beer; II – 1:10 diluted; III – 1:5 diluted; IV – 1:1 diluted; C-values: $C_{\text{I}} = 1.25 \pm 0.14$ nM; $C_{\text{II}} = 1.83 \pm 0.2$ nM; $C_{\text{III}} = 2.75 \pm 0.22$ nM; $C_{\text{IV}} = 9.7 \pm 0.9$ nM). b) Results of the amperometric detection for 1:5 diluted OTA-spiked beer which was performed with a smartphone connected via Bluetooth to a miniaturized potentiostat. Error bars were obtained from three independent measurements.

approximately 5 times smaller than for the standard OTA samples, and the C-value increases to 9.7 ± 0.9 nM. To minimize the matrix effects a higher dilution of the beer of at least 1:5 has proven to be more appropriate. With a 1:5 and 1:10 dilution only a small loss of sensitivity could be observed. C-values of 2.75 ± 0.22 nM and 1.83 ± 0.20 nM were obtained, respectively and recovery rates of 138% for 1:5 and 117% for 1:10 diluted beer could be achieved. However, for the detection of small OTA concentrations in real beer samples, a high dilution should be prevented. Therefore, we continued our investigations with 1:5 diluted beer. To test the applicability for on-site measurements, we have miniaturized the set-up using a handheld potentiostat, which can be controlled with a smartphone via Bluetooth. Compared to the traditional bench-top potentiostat, we could not find any disadvantages of the amperometric measurements and observed a similar signal-to-noise ratio. With 1:5 diluted OTA-spiked beer we were able to quantify an OTA content ranging from 1.25 nM to 12.5 nM ($\approx 0.5 \mu\text{g L}^{-1}$ to $5 \mu\text{g L}^{-1}$, see Figure 7b) using amperometric detection. Based on the limit values of other alcoholic beverages such as wine, which are as low as $2 \mu\text{g L}^{-1}$,^[2] the interesting measuring range would be covered. With this we demonstrate that amperometric detection can be used to develop a miniaturized detection system for the quantification of OTA. Further, this could be adopted to many other HRP-based enzyme-linked assays.

3. Conclusion

It could be demonstrated that the pH value and electrode material significantly control the electrochemistry of TMB. It was found that screen-printed gold electrodes and a highly acidic pH value (pH 1) are well-suited to perform the electrochemical detection of TMB, due to the reversible character of the redox reaction under these conditions.

In addition, it was shown that the electrode response is not changed by the electrochemical reaction, which enables to use

one electrode to measure multiple samples. In contrast to this, for carbon screen-printed electrodes, it was found that the electrode response has changed after the electrochemical reaction with TMB at pH 1. At a weakly acidic pH value (pH 4), neither with carbon nor with gold screen-printed electrodes a reproducible electrochemical detection of TMB could be achieved.

An amperometric detection system for oxidized TMB was therefore established with gold screen-printed electrodes and the detection was performed at pH 1. An immunomagnetic OTA assay was developed, in which an OTA-HRP tracer was applied. To quantify OTA, the enzymatic reaction of the tracer with TMB/ H_2O_2 was detected by amperometry and photometry and both detection methods are in good correlation. This gives great promise for the electrochemical detection of TMB in many other HRP-based assays. It provides a straight-forward approach to move from optical to electrochemical detection, since many assays are already optimized for the TMB-based optical detection. Furthermore, we have demonstrated the applicability of the immunomagnetic assay for OTA spiked beer. Here we were able to quantify OTA down to $0.5 \mu\text{g L}^{-1}$ in beer by amperometric detection with a handheld potentiostat connected via Bluetooth to a smartphone. The developed amperometric detection system is therefore highly promising to connect HRP-based assays with smart technologies and it represents a miniaturized and low-cost alternative to optical TMB detection.

Experimental Section

Materials

TMB 3,3', 5, 5'-Tetramethylbenzidine and TweenTM 20 were obtained from Serva Electrophoresis GmbH (Heidelberg, Germany). DynabeadsTM Protein G for Immunoprecipitation were purchased from InvitrogenTM, (Thermo Fisher Scientific, Inc., Massachusetts, US). Screen-printed gold (250AT) and carbon electrodes (110) were obtained from Metrohm DropSens (Herisau, Swiss). Ochratoxin A from *Petromyces albertensis*, $\geq 98\%$ (HPLC); sodium citrate monobasic BioXtra, anhydrous, $\geq 99.5\%$; sodium chloride BioUltra, $\geq 99.5\%$; potassium phosphate dibasic anhydrous, BioUltra, $\geq 99.0\%$; N,N'-dicyclohexylcarbodiimide (DCC) for synthesis; Tri-fluoroacetic acid ReagentPlus[®], 99%; N,N'-Disuccinimidyl carbonate (DSC) $\geq 95\%$; N,N-Dimethylformamide anhydrous (DMF), 99.8%; N,N-Dimethylacetamide (DMA), 99.8%; Sulfuric acid ACS reagent, 95.0–98.0%; Tris(hydroxymethyl)aminomethane (TRIS), Millipore[®]; dihydroxyacetone phosphate (DHAP); acetonitrile anhydrous, 99.8%; disodium hydrogen phosphate dihydrate Potassium phosphate monobasic $\geq 99.0\%$; dipotassium hydrogen phosphate $\geq 99\%$; sodium dihydrogen phosphate dihydrate $\geq 99\%$; potassium sorbate purum p.a., $\geq 99.0\%$; N-hydroxysuccinimide 98% (NHS) and hydrogen peroxide solution $\geq 30\%$, for trace analysis were purchased from Sigma Aldrich (now Merck KGaA, Darmstadt, Germany). Primary mouse monoclonal IgG anti-OTA antibodies from different cell clones (CH2 0.42 mg mL^{-1} ; BG4 1 mg mL^{-1} ; BC10 0.5 mg mL^{-1}) were provided by Hybrotec GmbH (Potsdam, Germany). Secondary polyclonal sheep anti-mouse IgG antibodies IgG (R1256P) were obtained from Acris Antibody GmbH, (Herford, Germany). Potassium hexacyanoferrate(III), 98 + % ($\text{K}_3[\text{Fe}(\text{CN})_6]$) and potassium chloride, ACS, 99.0–100.5% from Alfa Aesar Co.Inc.

(Massachusetts, US) were used. Pilsner-type beer was degassed by filters (Whatman® qualitative filter paper, Grade 1 circles, diam. 150 mm). Transparent 96-well microplates UV Star® from Greiner Bio-One GmbH (Solingen, Germany) were used for ELISA and transparent non-binding 96-well microplates were used for immunomagnetic OTA assays. A desalting Sephadex-G25 PD10-column was purchased from GE Healthcare Life Sciences (Germany). Horseradish peroxidase (HRP) with EIA grade from Roche (Mannheim, Germany) was applied for the tracer synthesis. Ultrapure water was obtained from a Milli-Q water purification system (Millipore, Bedford, MA, USA).

Cyclic Voltammetry

Cyclic voltammetry measurements were performed with a potentiostat (Autolab PGSTAT101, Metrohm AG – Herisau, Switzerland) in a custom-made wall-jet flow cell, fabricated of poly(methyl methacrylate) (see Figures S19 and S20), while the flow was interrupted. All potentials were applied vs. the pseudo Ag/AgCl reference electrode and the measurements were performed at room temperature (RT). To investigate the electrochemistry of TMB at pH 4, screen-printed gold and carbon electrodes were analysed by cyclic voltammetry in buffer (220 mM sodium citrate buffer with 100 mM KCl, pH 4). Five cycles were recorded for each electrode. The same electrodes were used to perform cyclic voltammetry measurements with TMB. Therefore, 30 cycles were performed in buffer with 500 μM TMB. Afterwards, the electrodes were rinsed by flushing 3 mL of the buffer through the flow cell. Finally, cyclic voltammetry was performed again in buffer for 5 cycles to compare it with the initial measurement. For the studies of the electrochemistry of TMB at pH 1 at the screen-printed gold and carbon electrodes, the above described measurements were repeated in 150 mM sodium citrate buffer with 300 mM H_2SO_4 and 100 mM KCl (pH 1) and 500 μM TMB.

Tracer Synthesis

The OTA-HRP tracer was synthesized by DCC/NHS activation of the carboxylic group of OTA and subsequent binding to amino groups of the HRP. A 0.5 M stock solution each of NHS and DCC was prepared and used immediately for the reaction. 6 μmol of OTA were dissolved in 15 μL DMF. In the following order, 7.2 μmol NHS, 3.9 μmol DSC and 7.2 μmol DCC were added. The reaction mixture was incubated under shaking over night with 800 rpm at RT with a ThermoMixer (Eppendorf, Germany). Afterwards, the mixture was centrifuged with 10000 G, and the supernatant was used for the reaction with HRP. Therefore, 2.2 mg HRP were dissolved in 250 μL 0.13 M NaHCO_3 and cooled down to 2 °C. Gradually, 9 μL of NHS-OTA-ester were added. Under constant shaking every 5 min 3 μL were added. The mixture was shaken for 3 h at 2 °C. For separation of the tracer, gel permeation chromatography with a Sephadex-G25 PD10-column was performed. For equilibration, the column was filled with 25 mL 1:10 diluted PBS (pH 7.6). Subsequently the reaction mixture was given on the column, and the sample was eluted with 7.5 mL of 1:10 diluted PBS (pH 7.6). The eluate was collected with a transparent microplate with three drops per fraction and analysed with UV/Vis measurements at a wavelength of 405 nm, referenced to 280 nm. The three fractions with the highest optical density were combined and stored at 4 °C. The HRP concentration was determined with a calibration of HRP standards and UV/Vis measurements at a wavelength of 405 nm, referenced to 280 nm. The coupling density was determined with MALDI-TOF/MS as described in the Supporting Information.

OTA ELISA

Transparent high-binding 96-well microtiter plates were used for the direct competitive OTA ELISA with HRP as label and TMB/ H_2O_2 as enzymatic substrates. All incubation steps were performed under shaking at 750 rpm on a Titramax 101 plate shaker (Heidolph, Schwabach, Germany) and RT. The washing of the microplates was performed with wash buffer (0.75 mM potassium dihydrogen phosphate, 6.25 mM dipotassium hydrogen phosphate, 0.025 mM sorbic acid potassium salt, 0.05% (v/v) Tween™ 20, pH 7.6) by a plate washer (BioTek Instruments, ELx405 Select™, Bad Friedrichshall, Germany) with three cycles per washing step.

Initially, 200 μL of secondary sheep anti-mouse antibody (1 mg mL^{-1} in PBS, pH 7.6) were added to each well and incubated for 16 h. Afterwards, the plate was washed and coated with primary mouse-anti OTA IgG antibodies (CH2, BG4 or BC10). Therefore, 200 μL of antibody in PBS (pH 7.6) were added per well (with optimized antibody concentrations for CH2: 42 ng mL^{-1} , BG4: 25 ng mL^{-1} and BC10: 25 ng mL^{-1}). After one hour of incubation, the plate was washed with PBS Tween (0.05% Tween). Subsequently, 150 μL of OTA standard solutions in Tris buffer (10 mM Tris, 150 mM NaCl) with concentrations ranging from 1 ng L^{-1} to 1 mg L^{-1} , and 50 μL of OTA-HRP tracer were added (with optimized tracer concentrations with 180 ng mL^{-1} for CH2, 45 ng mL^{-1} for BG4 and 90 ng mL^{-1} for BC10). After 30 min of incubation, the microplate was washed again. Thereafter, 200 μL of TMB/ H_2O_2 substrate solution (360 μM TMB, 3.7 mM H_2O_2 in 220 mM sodium citrate buffer, pH 4) were added and incubated for 20 min. Finally, the enzymatic reaction was stopped with 100 μL of 1 M H_2SO_4 per well and the OD was measured at a wavelength of 450 nm referenced to 620 nm.

Immunomagnetic OTA Assay

Transparent non-binding 96-well microtiter plates were used for the direct competitive immunomagnetic OTA assay. Protein G decorated magnetic beads were used as a platform to immobilize the primary anti-OTA mouse IgG antibody (BG4). All incubation steps were performed under shaking at 1000 rpm on a Titramax 101 plate shaker (Heidolph, Schwabach, Germany) and RT. The washing steps were performed by manually adding and removing wash buffer (0.75 mM potassium dihydrogen phosphate, 6.25 mM dipotassium hydrogen phosphate, 0.025 mM sorbic acid potassium salt, 0.05% (v/v) Tween™ 20, pH 7.6) with a multi-channel pipette to each well containing magnetic beads. For each washing step the beads were magnetically captured with a plate separator (BioMag® 96-Well Plate Separator, Polysciences, Inc., Warrington, PA, USA) and washed three times with wash buffer.

Initially, 40 μL of the magnetic beads (30 mg mL^{-1}) were used for a single assay with 96 samples. In a 1.5 mL reaction tube, the beads were captured with a magnet, and the supernatant was removed. Afterwards, 200 μL PBS and 1 μg of antibodies (anti-OTA mouse IgG, BG4) were added and incubated under shaking with a ThermoMixer (Eppendorf, Germany) at 1000 rpm and RT for 30 min. The beads were washed three times with wash buffer and subsequently dispersed in 12 mL Tris buffer (10 mM Tris, 150 mM NaCl). To each well 100 μL of magnetic bead dispersion were added, and the supernatant was removed under magnetic capturing. Thereafter, the beads were incubated with 150 μL of OTA standard solutions in Tris buffer (10 mM Tris, 150 mM NaCl) with concentrations ranging from 1 ng L^{-1} to 1 mg L^{-1} and 50 μL of OTA-HRP tracer (44 ng mL^{-1}) for 30 min. Subsequently, the beads were washed and incubated with 200 μL per well of TMB/ H_2O_2 substrate solution (360 μM TMB, 3.7 mM H_2O_2 in 220 mM sodium citrate buffer, pH 4). To stop the reaction and to adjust the Cl^- concentration of the samples to 100 mM for amperometric

measurements, 100 μL of 1 M H_2SO_4 with 300 mM KCl were added to each well. Similar as for the OTA ELISA, the OD was measured at a wavelength of 450 nm, referenced to 620 nm. Finally, amperometric measurements with each sample could be performed as described below.

Preparation of Beer Samples

Pilsner-type beer samples were degassed by filtration with a Whatman® 1 filter and diluted 1:1, 1:5 or 1:10 with Tris buffer (10 mM Tris, 150 mM NaCl). Afterwards the samples were spiked with OTA resulting in concentrations ranging from 1 ng L^{-1} to 1 mg L^{-1} .

Amperometric Measurements

Amperometric measurements were performed with a potentiostat (Autolab PGSTAT101, Metrohm AG – Herisau, Switzerland) in the wall-jet flow cell with screen-printed gold electrodes and a flow rate of 600 $\mu\text{L min}^{-1}$. A syringe-pump (Bee Syringe Pump, BASi, IN, USA) was applied. To verify the applicability of the flow-cell for amperometry, measurements with potassium ferricyanide were performed. A potential of 0 V vs. Ag/AgCl, sufficiently low enough to reduce ferricyanide, was applied. Initially, 100 mM potassium phosphate buffer (pH 7) was flushed over the electrode, until the basic current reached a steady state. Subsequently, alternately with buffer, potassium ferricyanide samples with different concentrations ranging from 0.2 μM to 10 μM (in 100 mM potassium phosphate buffer, pH 7) were passed through the flow system until the redox current attained a steady state. To test the repeatability, each potassium ferricyanide sample was injected three times and the mean redox current was plotted vs. the concentration (see Figure S21). For the amperometric detection of oxidized TMB and to test the influence of TMB and H_2O_2 , the measurements were performed in the same manner as described above. Here a potential of 300 mV vs. Ag/AgCl was applied. To examine, if H_2O_2 and reduced TMB would give a redox current under the chosen experimental conditions amperometry with 5 mM H_2O_2 and 0.5 mM TMB was performed with 150 mM sodium citrate buffer with 300 mM H_2SO_4 and 100 mM KCl (see Figure S22). To avoid any error, 3.7 mM H_2O_2 and 360 μM TMB, as used for the immunoassays, was added to the running buffer. The detection step of the OTA assay in beer samples was performed with a handheld potentiostat EmStat3 Blue (PalmSens, Netherlands) connected via Bluetooth to an android smartphone (Samsung).

Acknowledgements

Financial support from BAM for the focus area project (Themenfeldprojekt) TF20 is kindly acknowledged. The antibody development was funded by the German Federal Ministry of Education and Research (BMBF) within the project “KOMBI-SPEC”, contract no. 13 N13759. We greatly thank Robert Tannenber for the photography of the set up. We would like to thank Dr. Jérôme Bell and Alexander Ecke for the scientific discussions. The authors acknowledge Dr. Francesca Mirabella for technical support with ToF-SIMS measurements. We are also extremely grateful to Christoph Naese for the high-precision production of the flow cell. Further thanks go to Sigrid Benemann for taking scanning electron microscopy images. We would also like to thank Dr. Marc Riedel for the active support with proofreading and the scientific

discussions. Open access funding enabled and organized by Projekt DEAL.

Conflict of Interest

The authors declare no conflict of interest.

Keywords: amperometry · cyclic voltammetry · immunoassays · screen-printed electrodes · 3,3',5,5'-tetramethylbenzidine

- [1] B. A. Al Jaal, M. Jaganjac, A. Barcaru, P. Horvatovich, A. Latiff, *Food Chem. Toxicol.* **2019**, *129*, 211–228.
- [2] COMMISSION REGULATION (EC) No 1881/2006, **2006**, L 364/5, 1–20.
- [3] A. Mally, W. Dekant, *Mol. Nutr. Food Res.* **2009**, *53*, 467–478.
- [4] A. Pfohl-Leszczkovic, R. A. Manderville, *Chem. Res. Toxicol.* **2012**, *25*, 252–262.
- [5] V. Sava, O. Reunova, A. Velasquez, R. Harbison, J. Sanchez-Ramos, *Neurotoxicology* **2006**, *27*, 82–92.
- [6] L. Al-Anati, E. Petzinger, *J. Vet. Pharmacol. Ther.* **2006**, *29*, 79–90.
- [7] a) C. Tessini, C. Mardones, D. von Baer, M. Vega, E. Herlitz, R. Saelzer, J. Silva, O. Torres, *Anal. Chim. Acta* **2010**, *660*, 119–126; b) G. J. Soleas, J. Yan, D. M. Goldberg, *J. Agric. Food Chem.* **2001**, *49*, 2733–2740; c) A. Visconti, M. Pascale, G. Centonze, *J. Chromatogr. A* **1999**, *864*, 89–101; d) Z. M. Zheng, J. Hanneken, D. Houchins, R. S. King, P. Lee, J. L. Richard, *Mycopathologia* **2005**, *159*, 265–272.
- [8] Y. Y. Jiao, W. Blas, C. Ruhl, R. Weber, *J. Chromatogr.* **1992**, *595*, 364–367.
- [9] K. Thirumala-Devi, M. A. Mayo, G. Reddy, S. V. Reddy, P. Delfosse, D. V. R. Reddy, *J. Agric. Food Chem.* **2000**, *48*, 5079–5082.
- [10] J. Wang, *Chem. Rev.* **2008**, *108*, 814–825.
- [11] a) A. P. F. Turner, B. N. Chen, S. A. Piletsky, *Clin. Chem.* **1999**, *45*, 1596–1601; b) J. D. Newman, A. P. F. Turner, *Biosens. Bioelectron.* **2005**, *20*, 2435–2453; c) L. A. Zhang, C. C. Gu, H. Ma, L. L. Zhu, J. J. Wen, H. X. Xu, H. Y. Liu, L. H. Li, *Anal. Bioanal. Chem.* **2019**, *411*, 21–36.
- [12] a) X. P. Liu, Y. J. Deng, X. Y. Jin, L. G. Chen, J. H. Jiang, G. L. Shen, R. Q. Yu, *Anal. Biochem.* **2009**, *389*, 63–68; b) J. C. Vidal, L. Bonel, P. Duato, J. R. Castillo, *Anal. Methods* **2011**, *3*, 977–984; c) J. C. Vidal, L. Bonel, F. A. Ezquerra, P. Duato, J. R. Castillo, *Anal. Bioanal. Chem.* **2012**, *403*, 1585–1593; d) A. Jodra, M. Hervas, M. A. Lopez, A. Escarpa, *Sens. Actuators B* **2015**, *221*, 777–783; e) P. R. Perrotta, F. J. Arevalo, N. R. Vettorazzi, M. A. Non, H. Fernandez, *Sens. Actuators B* **2012**, *162*, 327–333; f) A. E. Radi, X. Munoz-Berbel, V. Lates, J. L. Marty, *Biosens. Bioelectron.* **2009**, *24*, 1888–1892.
- [13] a) L. Rivas, C. C. Mayorga-Martinez, D. Quesada-Gonzalez, A. Zamora-Galvez, A. de la Escosura-Muniz, A. Merkoci, *Anal. Chem.* **2015**, *87*, 5167–5172; b) G. Castillo, I. Lamberti, L. Mosiello, T. Hianik, *Electroanalysis* **2012**, *24*, 512–520; c) J. J. Wu, H. Q. Chu, Z. L. Mei, Y. Deng, F. Xue, L. Zheng, W. Chen, *Anal. Chim. Acta* **2012**, *753*, 27–31.
- [14] J. G. Pacheco, M. Castro, S. Machado, M. F. Barroso, H. P. A. Nows, C. Delerue-Matos, *Sens. Actuators B* **2015**, *215*, 107–112.
- [15] V. Koh, W. L. Ang, A. Bonanni, *ChemElectroChem* **2018**, *5*, 3654–3659.
- [16] a) A. A. v. d. D. E. S. Bos, N. van Rooy, A. H. W. M. Schuurs, *J. Immunoassay* **1981**, *2*, 187–204; b) T. Porstmann, S. T. Kiessig, *J. Immunol. Methods* **1992**, *150*, 5–21.
- [17] P. D. Josephy, T. Eling, R. P. Mason, *J. Biol. Chem.* **1982**, *257*, 3669–3675.
- [18] Y. Misono, Y. Ohkata, T. Morikawa, K. Itoh, *J. Electroanal. Chem.* **1997**, *436*, 203–212.
- [19] a) G. Y. Lee, J. H. Park, Y. W. Chang, S. Cho, M. J. Kang, J. C. Pyun, *Anal. Chim. Acta* **2017**, *971*, 33–39; b) G. Volpe, D. Compagnone, R. Draisci, G. Pallechi, *Analyst* **1998**, *123*, 1303–1307; c) S. Amaya-Gonzalez, N. delos-Santos-Alvarez, M. J. Lobo-Castan, A. J. Miranda-Ordieres, P. Tunon-Blanco, *Electroanalysis* **2011**, *23*, 108–114; d) P. Fanjul-Bolado, M. B. Gonzalez-Garia, A. Costa-Garcia, *Anal. Bioanal. Chem.* **2005**, *382*, 297–302; e) J. J. Ezenarro, N. Parraga-Nino, M. Sabria, F. J. Del Campo, F. X. Munoz-Pascual, J. Mas, N. Uria, *Biosensors* **2020**, *10*, 1–11; f) J. Barallat, R. Olive-Monllau, J. Gonzalo-Ruiz, R. Ramirez-Satorras, F. X. Munoz-Pascual, A. G. Ortega, E. Baldrich, *Anal. Chem.* **2013**, *85*, 9049–9056; g) A. Crew, C. Alford, D. C. C. Cowell, J. P. Hart, *Electrochim. Acta* **2007**, *52*, 5232–5237.

- [20] A. E. Radi, X. Munoz-Berbel, M. Cortina-Puig, J. L. Marty, *Electrochim. Acta* **2009**, *54*, 2180–2184.
- [21] a) J. S. del Rio, O. Y. F. Henry, P. Jolly, D. E. Ingber, *Nat. Nanotechnol.* **2019**, *14*, 1143–+; b) M. L. Liu, Y. Y. Zhang, Y. D. Chen, Q. J. Xie, S. Z. Yao, *J. Electroanal. Chem.* **2008**, *622*, 184–192.
- [22] L. Björck, G. Kronvall, *J. Immunol.* **1984**, *133*, 969–974.
- [23] A. Frey, B. Meckelein, D. Externest, M. A. Schmidt, *J. Immunol. Methods* **2000**, *233*, 47–56.
- [24] W. J. Yang, H. Y. Zhang, M. X. Li, Z. H. Wang, J. Zhou, S. H. Wang, G. D. Lu, F. F. Fu, *Anal. Chim. Acta* **2014**, *850*, 85–91.
- [25] T. Schmid, P. Dariz, *Heritage* **2019**, *2*, 1662–1683.
- [26] A. H. Heussner, L. E. Bingle, *Toxin Rev.* **2015**, *7*, 4253–4282.

Manuscript received: April 2, 2021

Revised manuscript received: June 8, 2021

Accepted manuscript online: June 8, 2021